Published in final edited form as:
Curr Microbiol. 2011 April ; 62(4): 1321–1330. doi:10.1007/s00284-010-9862-4.

Transcriptomic Analysis for Genetic Mechanisms of the Factors Related to Biofilm Formation in Escherichia coli O157:H7

Jin-Hyung Lee[a], **Yong-Guy Kim**[a], **Moo Hwan Cho**[a], **Thomas K. Wood**[b,*], and **Jintae Lee**[a,*]

[a]School of Display & Chemical Engineering, Yeungnam University, Gyeongsan-si Gyeongsangbuk-do, 712-749, Korea

[b]Department of Chemical Engineering, 220 Jack E. Brown Building, Texas A & M University, College Station, TX 77843-3122, USA

Abstract

Two lineages of enterohemorrhagic *Escherichia coli* O157:H7 (EDL933, $Stx1^+$ and $Stx2^+$) and 86-24 ($Stx2^+$) were investigated to determine the genetic basis of biofilm formation on abiotic surfaces. Strain EDL933 formed a robust biofilm while strain 86-24 formed almost no biofilm on either polystyrene plates or polyethylene tubes. Whole-transcriptome profiles of EDL933 vs. 86-24 revealed that in the strong biofilm-forming strain, genes involved in curli biosynthesis (*csgBAC* and *csgDEFG*) and cellulose production (*adrA*) were significantly induced, whereas genes involved in indole signaling (*trpLED* and *mtr*) were most repressed. Additionally, 49 phage genes were highly induced and repressed between the two strains. Curli assays using Congo red plates and scanning electron microscopy corroborated the microarray data as the EDL933 strain produced a large amount of curli, while strain 86-24 formed much less curli. Moreover, EDL933 produced 19-fold more cellulose than 86-24, and indole production in EDL933 was two times lower than that of the strain 86-24. Therefore, it appears *E. coli* O157:H7 EDL933 produces more biofilm because of its increased curli and cellulose production and reduced indole production.

Keywords

biofilm; curli; indole; *Escherichia coli* O157:H7

1. Introduction

Enterohemorrhagic *Escherichia coli* serotype O157:H7 is the most common human pathogen responsible for outbreaks of hemorrhagic colitis causing bloody diarrhea that can lead to the life-threatening hemolytic-uremic syndrome that affects mostly children around the world (Boyce et al., 1995). Understanding *E. coli* O157:H7 infections is important given that there are approximately 73,000 infections annually in the U.S., directly leading to 2,000 hospitalizations, 60 deaths, and an economic cost up to $405 million (in 2003 dollars) (Frenzen et al., 2005).

Depending on the specific strain, *E. coli* serotype O157:H7 can produce both Shiga toxin 1 (Stx1) and 2 (Stx2) that are responsible for hemorrhagic colitis (Nataro & Kaper 1998). It has a very low infectious dose (as low as 50 CFU in one outbreak) and colonizes the intestinal epithelial cells, where it causes attaching and effacing lesions (Nataro & Kaper 1998). *E. coli* serotype O157:H7 strain EDL933 was implicated in two outbreaks of

*Corresponding author: Jintae Lee, jtlee@ynu.ac.kr, Phone: 82-53-810-2533, Fax: 82-53-810-4631. *Co-corresponding author: Thomas K. Wood, Thomas.Wood@chemail.tamu.edu, Phone: (979) 862-1588, Fax: (979) 865-6446.

hemorrhagic colitis in the USA during 1982 (Wells et al., 1983) and produces both Stx1 and Stx2 toxins (Strockbine et al., 1986). *E. coli* O157:H7 strain 86-24, caused a hemorrhagic colitis outbreak in the USA during 1986 (Griffin et al., 1988) and produces only Stx2 (Jarvis & Kaper 1996). Epidemiological data suggest that Stx2 is more important than Stx1 in the development of hemolytic-uremic syndrome (Griffin 1995), although this result is not conclusive because, unlike Stx1, Stx2 has many variants (Nataro & Kaper 1998).

Bacterial biofilms are ubiquitous in natural, medical, and engineering environments (Potera 1999). Biofilms have been associated with many chronic infections such as prostatitis, biliary tract infections, and urinary catheter cystitis by pathogenic *E. coli* due to their high resistance to antimicrobial agents (Costerton et al., 1999). Food-borne microorganisms, such as *E. coli* O157:H7, can readily attach to and form biofilms on various surfaces, such as stainless steel, glass, and polystyrene (Ryu & Beuchat 2005, Rivas et al., 2007). The genetic mechanism of biofilm formation of *E. coli* O157:H7 is a complex process and is now beginning to be unveiled. The production of curli fimbriae (Ryu & Beuchat 2005, Uhlich et al., 2006, Saldaña et al., 2009) is the most common contributor to the biofilm formation in *E. coli* O157:H7. Diverse proteins also play an important role in the biofilm formation of *E. coli* O157:H7 (Wells et al., 2008, Puttamreddy et al., 2010, Lee et al., 2008b). Additionally, intercellular signal molecules, such as autoinducer-2 (Yoon & Sofos 2008, Bansal et al., 2008) and indole (Lee et al., 2007, Lee & Lee 2010), are involved in biofilm formation of *E. coli* O157:H7.

In this study, we initially observed a significant difference in the biofilm formation of the two *E. coli* O157:H7 strains, EDL933 and 86-24. DNA microarrays were utilized to identify the genetic basis for this difference in biofilm formation. Global gene expression from the microarray data was corroborated by phenotypic assays including those for curli, cellulose, and indole. It was found that EHEC biofilm formation depends chiefly on enhanced curli and cellulose production along with reduced indole production.

2. Materials and Methods

Bacterial strains, materials, and growth rate measurements

Two pathogenic strains of enterohemorrhagic *E. coli* O157:H7, strain EDL933 (ATCC43895) (Strockbine et al., 1986)) and strain 86-24 (kindly provided by Dr. Arul Jayaraman of Texas A&M University) (Griffin et al., 1988) were used. EDL933 was sequenced (Perna et al., 2001), whereas the strain 86-24 has not been sequenced. Luria-Bertani medium (LB) (Sambrook et al., 1989) was used for growth. All chemicals (Congo red, Coomasie brilliant blue, indole, calcofluor, crystal violet, sodium phosphate, and β-mercapto ethanol) were purchased from Sigma-Aldrich Co. (Missouri, USA). Glutaraldehyde, formaldehyde, acetonitrile, amyl alcohol, ethyl alcohol, hydrochloric acid, OsO4, and ρ-dimethylamino-benzaldehyde were purchased from Junsei Chemical Co. (Tokyo, Japan) or Duksan Pure Chemical Co. (Ansan, Korea). All experiments were performed with LB medium at 37°C (human body temperature). The strains were initially streaked from −80°C glycerol stocks and a fresh single colony was inoculated 25 ml LB medium in 250 ml flasks and cultured at 250 rpm. Overnight cultures were diluted 1:100 using LB medium. For cell growth measurements, the turbidity was measured at 600 nm (OD_{600}) with a spectrophotometer (UV-160, Shimadzu, Japan). When the value of OD_{600} was above 0.7, the culture sample was diluted into the linear range of 0.2 to 0.7. Each experiment was performed with at least two independent cultures.

Crystal-violet biofilm assay

A static biofilm formation assay was performed in 96-well polystyrene plates (SPL life sciences, Korea) or 14 mL polyethylene test tubes (SPL life sciences) as previously reported (Pratt & Kolter 1998). Briefly, cells were inoculated at an initial turbidity at 600 nm of 0.05 for 24 h without shaking. Cell growth and total biofilm were measured using crystal violet staining. Each data point was averaged from at least twelve replicate wells (six wells from each of at least two independent cultures).

Total RNA isolation

For the microarray experiments, planktonic cells of EDL933 and 86-24 were cultured to a turbidity of 4.0 at 600 nm. Due to the very low biofilm formation of 86-24, planktonic cells were used to study the whole transcriptome profiles. Cells were immediately chilled with dry ice and 95% ethanol (to prevent RNA degradation) for 30 sec before centrifugation at 13,000 g for 2 min; cell pellets were frozen immediately with dry ice and stored −80°C. RNA was isolated using Qiagen RNeasy mini Kit described previously (Ren et al., 2004).

DNA Microarray analysis

The *E. coli* GeneChip Genome 2.0 Array (Affymetrix, P/N 900551, Santa Clara, USA) was used to study the differential gene expression profile for EDL933 vs. 86-24 as described in the Gene Expression Technical Manual. Ten μg of total RNA from each sample was converted to cDNA using random primers. The purified cDNA was fragmented using 0.6 U/μg of DNAse I and end-labeled by terminal transferase reaction incorporating a biotinylated dideoxynucleotide. Hybridization was performed for 16 hours at 45°C and 60 rpm as described in the GeneChip Expression Analysis Technical Manual (Affymetrix). After hybridization, the chips were stained and washed in a GeneChip Fluidics Station 450 (Affymetrix) and scanned by using a GeneChip Array scanner 3000 7G (Affymetrix), and the total cell intensity was scaled automatically in the software to an average value of 500. The probe array images were inspected for any image artifact. Background values, noise values, and scaling factors of both arrays were examined and were comparable. The intensities of the polyadenosine RNA controls of Bacillus subtilis (*lys*, *phe*, *thr*, and *dap*) at different concentrations were used to monitor the labeling and scanning process. A gene was considered differentially expressed when the p-value for comparing two chips was lower than 0.05 (to assure that the change in gene expression was statistically significant and that false positives arise less than 5%) and when the expression ratio was higher (3-fold) than the standard deviations for whole microarray (2.6-fold). Gene functions were obtained from the Affymetrix–NetAffx Analysis Center (https://www.affymetrix.com/analysis/netaffx/index.affx).

Quantitative real-time reverse transcription polymerase chain reaction (qRT-PCR)

To corroborate the DNA microarray data and curli assay and to confirm the induction of indole production, qRT-PCR was used to investigate the transcription level of *csgA* (encoding a curlin major subunit) and *tnaA* (encoding indole-synthesizing tryptophanase) using two independent RNA samples. Two primers for *csgA* (forward primer 5′-AGATGTTGGTCAGGGCTCAG-3′ and reverse primer 5′-CGTTGTTACCAAAGCCAACC-3′) and two primers for *tnaA* (forward primer 5′-TACACCATTCCGACTCACCA-3′ and reverse primer 5′-CCGTATCGAAGGCTTCTTTG-3′) were used. The expression level of the housekeeping gene *rrsG* (16S rRNA, forward primer 5′-TATTGCACAATGGGCGCAAG-3′ and reverse primer 5′-ACTTAACAAACCGCCTGCGT-3′) was used to normalize the expression data of interesting genes. The method of qRT-PCR was adapted (Lee et al., 2008a). qRT-PCR was

performed with SYBR Green master mix (Applied Biosystems, Foster City, USA) and ABI 7500 Real-Time PCR System (Applied Biosystems).

Curli assay

To measure curli production, Congo red plates (LB agar medium containing 20 μg/ml Congo red and 10 μg/ml Coomassie brilliant blue, and 15 g/L agar) were used as described previously to visualize curli production after 24 h incubation (Reisner et al., 2006). In order to corroborate the plate assay, scanning electron microscopy (SEM) was used by modifying the protocol (Hossain et al, 1995). Briefly, *E. coli* cells were cultured until a turbidity of 2.0 at 600 nm, and cells were directly fixed by adding glutaraldehyde (2.5% final) and formaldehyde (2% final) and incubated at 4°C overnight. Fixed cells were collected by filtering with a 0.45 μm nylon filter (Nalgene, New York, USA) with vacuum. The filter containing cells was cut into 0.5 × 0.5 mm squares and washed with 0.2 M sodium phosphate buffer before fixating for 90 min with osmium solution (containing 1.5 mL of sodium phosphate buffer 0.2 M, 3 mL of 2% OsO_4 and 3 mL deionized water). Then, samples were washed and dehydrated by successive 10 min incubations in 50% ethanol, 70% ethanol, 80% ethanol, 90% ethanol, and 95% ethanol followed by two successive incubations for 20 min in 100% ethanol. After dehydrating, the filters with cells were incubated in isoamyl acetate for 20 min and dried with critical-point dryer (HCP-2, Hitachi, Japan). The nylon filters were affixed to SEM stubs and coated with white gold for 200 seconds using ion sputtering (E-1030, Hitachi). The specimens were examined using the SEM S-4100 (Hitachi, Tokyo, Japan). The voltage was set at 15 kV and viewed at a magnification from x 2,000 to x15,000.

Cellulose assay

A cellulose assay using calcofluor (Ma & Wood 2009) was used. Cells (2 ml) at a turbidity of 4 were centrifuged and re-suspended in 1 ml of 1% tryptone with 16 mg/ml calcofluor and incubated for 2 h at 250 rpm. Bacterial bound calcofluor was removed by centrifugation for 5 min at 17 000 *g*, and the amount of calcofluor unbound to cellulose was determined by measuring the absorbance of the supernatant at 350 nm.

Indole assay

To measure the concentration of extracellular indole, EDL933 and 86-24 were grown to a turbidity of 4.0 at 600 nm. The turbidity of 4.0 represents the time point of the stationary phase at which the DNA microarray samples were taken. Indole concentrations were measured with the previous protocol using the Kovac's reagent (Kawamura-Sato et al., 1999). Briefly, Kovac's reagent (0.4 mL) was mixed with supernatants (1 mL) of bacterial cultures. The reaction mixture was diluted 1:10 in HCl-amyl alcohol solution (30 mL of HCl and 90 mL of amyl alcohol), and the absorbance of the mixture was measured at 540 nm with a spectrophotometer (Shimadzu UV-160). In addition, the spectrophotometric indole assay was corroborated with reverse-phase HPLC using a 100 × 4.6 mm Chromolith Performance RP-18e column (Merck KGaA, Darmstadt, Germany) and elution with H_2O-0.1% (v/v) trifluoroacetic acid and acetonitrile as the mobile phases at a flow rate of 0.5 mL/min (50:50). Under these conditions, the retention time and the absorbance maximum was 5.1 min/271 nm for indole.

3. Results

The main goal of this research was to investigate the genetic mechanism of biofilm formation of the two *E. coli* O157:H7 strains, EDL933 (good biofilm former) and 86-24 (poor biofilm former). DNA microarrays were initially utilized to predict the phenotypic

changes, and phenotypic assays for curli formation, cellulose, and indole production were performed to corroborate the whole transcriptome data.

Biofilm formation

Biofilm formation of the two *E. coli* O157:H7 strains was tested using 96-well polystyrene plates and polyethylene test tubes. While EDL933 formed robust biofilms, 86-24 formed almost no biofilm on both polystyrene plates (Fig. 1A) and polyethylene tubes (Fig. 1B). The specific growth rates of the two *E. coli* O157:H7 strains were almost identical (1.38 ± 0.07/h for EDL933 and 1.40 ± 0.08/h for 86-24); therefore, the changes in biofilm formation were not due to differences in growth rates.

Differential gene expression of EDL933 vs. 86-24

To investigate the global genetic basis for the difference in biofilm formation, DNA microarrays were used. For EDL933 vs. 86-24, 440 genes were differentially expressed more than 3-fold; 325 genes were induced and 115 genes were repressed. Partial lists of genes most induced and repressed are shown in the Table 1 and Table 2, and the whole set of expression data for the two strains has been deposited in the NCBI GENE Expression Omnibus and are accessible through accession number GSE 19953. As expected, 86-24 showed almost no signal for the *stx1B* and *stx1A* genes (Table 1) because strain 86-24 lacks Stx1 (Jarvis & Kaper 1996). Among the differentially expressed genes, many prophage genes of CP-933M, BP-933W, CP-933O, and CP-933V were highly induced in EDL933 (Table 1), whereas prophage genes of CP-933T were highly repressed in EDL933 (Table 2).

Among the most induced genes in EDL933 were seven curli genes (*csgBAC* and *csgDEFG*) (17- to 84-fold) (Table 1). Among the most repressed genes in EDL933 were, *trpLED*, involved in tryptophan synthesis (a substrate required for indole synthesis), and *mtr*, involved in indole-and tryptophan-uptake (Table 2).

Curli formation

Curli formation is important for biofilm formation for *E. coli* O157:H7 (Saldaña et al., 2009, Puttamreddy et al., 2010, Ryu & Beuchat 2005, Uhlich et al., 2006). Since the microarray data showed that seven curli genes (*csgBAC* and *csgDEFG*) were highly induced (Table 1), curli production was measured using Congo red plates and SEM. Congo red plates were used to observe the curli production with colonies grown under static conditions, while SEM images were used to examine the curli production from planktonic cells that were used for the DNA microarrays.

EDL933 produced a large amount of curli, whereas 86-24 produced almost no curli on the Congo red plate (Fig. 2A) and with SEM (Fig. 2B). For SEM, polymerized curli appeared as 4- to 7-nm wide fibers of varying lengths, and a large amount of curli appeared as a tangled and amorphous matrix surrounding bacterial cells (Chapman et al., 2002). EDL933 obviously produced a large amount of curli, while 86-24 produced few curli (Fig. 2B). These results corroborate well the microarray data (Table 1). Therefore, these results indicate that curli production is an important genetic mechanism of the different biofilm formation of the two *E. coli* O157:H7 strains. In addition, it is interesting that *E. coli* O157:H7 EDL933 is capable of making copious amounts of curli at 37°C whereas *E. coli* K-12 only makes curli at low temperatures(less than 32°C)(Gualdi et al., 2008).

Cellulose production

The curli protein CsgD also stimulates cellulose production directly by activating transcription of *adrA* (Zogaj et al., 2001) and also curli and cellulose play a synergistic role in biofilm formation (Saldaña et al., 2009). Since *adrA* was induced 8-fold in EDL933

(Table 1), cellulose production was measured for the two strains using cellulose specific calcofluor (Ma & Wood 2009). Indeed, EDL933 produced 19-fold more cellulose than 86-24 (0.57 ± 0.08 μg cellulose bound calcofluor/ml cells for EDL933 and 0.03 ± 0.06 μg cellulose bound calcofluor/ml cells for 86-24). Therefore, EDL933 produces much more of both curli and cellulose than 86-24.

Indole production

We discovered that extracellular indole inhibits the biofilm formation of *E. coli* O157:H7 (Lee et al., 2007, Bansal et al., 2007). Since the whole-transcriptome analysis showed that indole-related genes (*trpLED* and *mtr*) were significantly repressed in EDL933 (Table 2), extracellular indole concentrations were measured for the two strains. Corroborating the microarray data, EDL933 produced 2-fold less extracellular indole than 86-24 (210 ± 10 μM for EDL933 vs. 430 ± 10 μM for 86-24). This result partially explains the difference in biofilm formation for these two strains.

Confirmation of the microarray data

qRT-PCR was used to investigate the transcription of *csgA* (encoding a curlin major subunit) and *tnaA* (encoding indole-synthesizing tryptophanase). The qRT-PCR results were comparable with the DNA microarray data for *csgA* (10.2 ± 0.1-fold induction via qRT-PCR vs. 49-fold in the microarrays). Additionally, qRT-PCR showed 2.6 ± 0.4-fold lower of *tnaA* expression with EDL933 than 86-24, which corroborated the enhanced indole production in the EDL933.

4. Discussion

DNA microarrays have been utilized extensively to obtain whole-transcriptome profiling. For example, two separate lineages of *E. coli* O157:H7 were compared (EDL933 strains LI and LII) to determine if there are differences in expression of virulence-related genes (Dowd & Ishizaki 2006). They found differential expression of *stx2b*, *ureD*, curli (*csgAFEG*), stress-related genes (*hslJ*, *cspG*, *ibpB*, *ibpA*), type III secretion apparatus, LPS, and flagella under anaerobic conditions (Dowd & Ishizaki 2006). Here, we also used DNA microarrays to understand the genetic mechanisms of the biofilm formation of the two *E. coli* O157:H7 strains, EDL933 (ATCC43895) and 86-24.

In the current study, about 12% (440 genes) of the total genome (5416 genes, (Perna et al., 2001)) was differentially expressed (more than 3-fold). Among the highly induced and repressed genes (more than 6-fold), 49 prophage genes were identified (Table 1 and Table 2), which indicates the two tested strains have evolved differently. The antibiotic norfloxacin induces many prophage genes in the BP-933W prophage genome (Herold et al., 2005) including *z1443* through *z1469* (Table 1), and prophage genes play a role in *E. coli* K-12 biofilm formation (Wang et al., 2009). Also, the deletion of the *stx2* or the entire S*tx2*-encoding phage genes in the strain 86-24 did not affect *E. coli* O157:H7 colonization in sheep (Cornick et al., 2007). Therefore, it would be interesting to investigate whether the EDL933 specific prophage genes (Table 1) affect the biofilm formation and the antibiotic resistance of *E. coli* O157:H7.

The whole transcriptomic profiling showed that curli genes (*csgBAC* and *csgDEFG*), a cellulose gene (*adrA*), and indole-related genes (*trpLED* and *mtr*) are the most differentially expressed loci between the two strains (Table 1). The curli fibers produced by *E. coli* have many of the same biochemical and biophysical properties in common with human amyloid that is associated with Alzheimer's and prion diseases (Chapman et al., 2002), and curli formation is important for biofilm formation of pathogenic *E. coli* O157:H7 (Ryu & Beuchat

2005, Uhlich et al., 2006) as well as non-pathogenic *E. coli* (Prigent-Combaret et al., 2000, Landini 2009). Using a Congo red assay and SEM, this study confirmed that curli formation is an important positive factor for the biofilm formation of *E. coli* O157:H7 (Fig. 2AB). In agreement with this result, a study using transposon mutagenesis also showed that curli genes play a role in biofilm development in *E. coli* O157:H7 (Puttamreddy et al. 2010).

Corroborating the high expression of the cellulose gene *adrA* (Table 1), EDL933 produces 19-fold more cellulose than 86-24 although the expression of bacterial cellulose biosynthesis cluster (*bcsABZC*) was not changed in this transcriptome study. Cellulose production increases the binding of *E. coli* O157:H7 to sprouts (Matthysse et al., 2008) and increases biofilm formation in *E. coli* K-12 on hydrophilic surfaces, such as glass (Ma & Wood 2009). Also, cellulose production as well as curli production positively influence the biofilm formation of *E. coli* O157:H7 (Saldaña et al., 2009).

In addition, intercellular signal molecules, such as autoinducer-2 (Yoon & Sofos 2008) and indole (Lee et al., 2007, Bansal et al., 2007) are also be involved in biofilm formation of *E. coli* O157:H7. Since 86-24 produced more indole than EDL933 and formed almost no biofilm (Fig. 1), this result supports that elevated indole concentrations are partially responsible for the lack of biofilm formation by 86-24. Further support of this is that addition of 1 mM indole to EDL933 reduces its biofilm formation dramatically (Lee et al., 2007).

In the previous transcriptome study of the strong biofilm-forming strain EDL933, biofilm cells of EDL933 formed on glass wool repressed 20 pathogenic genes from the LEE island compared to planktonic cells of EDL933 which indicated that the virulence genes were not utilized in biofilm cells (Lee et al., 2007). The current study also could not identify any positive relationship between virulence gene expression and biofilm formation for the two *E. coli* O157:H7 strains. Hence, it is possible that environmental cues are missing that induce virulence genes under laboratory conditions within a single species.

To date, no effective therapy for *E. coli* O157:H7 serotypes has been found (Tarr et al., 2005, Boyce et al., 1995) because antibiotics, anti-motility agents, narcotics, and non-steroidal anti-inflammatory drugs are not usually provided as they increase the risk of developing hemolytic-uremic syndrome, a major cause of acute renal failure in children (Tarr et al., 2005); these agents induce an SOS response in *E. coli* O157:H7 which induces the prophage-based Shiga toxins (Kimmitt et al., 2000). Hence, controlling biofilm formation of *E. coli* O157:H7 is important in medicine as well as in food industry. In addition to antimicrobial therapy, anti-virulence therapies (Cegelski et al., 2008, Lesic et al., 2007) have been proposed because unlike antimicrobials, anti-virulence compounds do not affect growth and so there is less chance of developing resistance (Hentzer et al., 2002, Lesic et al., 2007). Since the two tested *E. coli* O157:H7 strains showed same growth rates but showed distinctive biofilm formation due to mainly curli and cellulose formation, controlling either curli formation or cellulose formation are possible ways to prevent biofilm formation of *E. coli* O157:H7.

Acknowledgments

This research was supported by the Yeungnam University research grant (to J. Lee). J-H. Lee and Y-G Kim were supported by the Brain Korea 21 Project from the Ministry of Education and Human Resources, Korea. T. Wood is the T. Michael O'Connor endowed chair and is also supported by the NIH (R01 GM089999).

References

Bansal T, Englert D, Lee J, Hegde M, Wood TK, Jayaraman A. Differential effects of epinephrine, norepinephrine, and indole on *Escherichia coli* O157:H7 chemotaxis, colonization, and gene expression. Infect Immun. 2007; 75:4597–4607. [PubMed: 17591798]

Bansal T, Jesudhasan P, Pillai S, Wood TK, Jayaraman A. Temporal regulation of enterohemorrhagic *Escherichia coli* virulence mediated by autoinducer-2. Appl Microbiol Biotechnol. 2008; 78:811–819. [PubMed: 18256823]

Boyce TG, Swerdlow DL, Griffin PM. *Escherichia coli* O157:H7 and the hemolytic-uremic syndrome. N Engl J Med. 1995; 333:364–368. [PubMed: 7609755]

Cegelski L, Marshall GR, Eldridge GR, Hultgren SJ. The biology and future prospects of antivirulence therapies. Nat Rev Microbiol. 2008; 6:17–27. [PubMed: 18079741]

Chapman MR, Robinson LS, Pinkner JS, Roth R, Heuser J, Hammar M, Normark S, Hultgren SJ. Role of *Escherichia coli* curli operons in directing amyloid fiber formation. Science. 2002; 295:851–855. [PubMed: 11823641]

Cornick NA, Helgerson AF, Sharma V. Shiga toxin and Shiga toxin-encoding phage do not facilitate *Escherichia coli* O157:H7 colonization in sheep. Appl Environ Microbiol. 2007; 73:344–346. [PubMed: 17085690]

Costerton JW, Stewart PS, Greenberg EP. Bacterial biofilms: a common cause of persistent infections. Science. 1999; 284:1318–1322. [PubMed: 10334980]

Dowd SE, Ishizaki H. Microarray based comparison of two *Escherichia coli* O157:H7 lineages. BMC Microbiol. 2006; 6:30. [PubMed: 16539702]

Frenzen PD, Drake A, Angulo FJ. Economic cost of illness due to *Escherichia coli* O157 infections in the United States. J Food Prot. 2005; 68:2623–2630. [PubMed: 16355834]

Griffin, PM. *Escherichia coli* O157:H7 and other enterohemorrhagic *Escherichia coli*. In: Blaser, PDSMJ.; Ravdin, JI.; Greenberg, HB.; Guerrant, RL., editors. Infections of the gastrointestinal tract. New York: Raven Press; 1995. p. 739-761.

Griffin PM, Ostroff SM, Tauxe RV, Greene KD, Wells JG, Lewis JH, Blake PA. Illnesses associated with *Escherichia coli* O157:H7 infections. A broad clinical spectrum. Ann Intern Med. 1988; 109:705–712. [PubMed: 3056169]

Gualdi L, Tagliabue L, Bertagnoli S, Ierano T, De Castro C, Landini P. Cellulose modulates biofilm formation by counteracting curli-mediated colonization of solid surfaces in *Escherichia coli*. Microbiology. 2008; 154:2017–2024. [PubMed: 18599830]

Hentzer M, Riedel K, Rasmussen TB, Heydorn A, Andersen JB, Parsek MR, Rice SA, Eberl L, Molin S, Høiby N, Kjelleberg S, Givskov M. Inhibition of quorum sensing in *Pseudomonas aeruginosa* biofilm bacteria by a halogenated furanone compound. Microbiology. 2002; 148:87–102. [PubMed: 11782502]

Herold S, Siebert J, Huber A, Schmidt H. Global expression of prophage genes in *Escherichia coli* O157:H7 strain EDL933 in response to norfloxacin. Antimicrob Agents Chemother. 2005; 49:931–944. [PubMed: 15728886]

Jarvis KG, Kaper JB. Secretion of extracellular proteins by enterohemorrhagic *Escherichia coli* via a putative type III secretion system. Infect Immun. 1996; 64:4826–4829. [PubMed: 8890245]

Kawamura-Sato K, Shibayama K, Horii T, Iimuma Y, Arakawa Y, Ohta M. Role of multiple efflux pumps in *Escherichia coli* in indole expulsion. FEMS Microbiol Lett. 1999; 179:345–352. [PubMed: 10518736]

Kimmitt PT, Harwood CR, Barer MR. Toxin gene expression by shiga toxin-producing *Escherichia coli*: the role of antibiotics and the bacterial SOS response. Emerg Infect Dis. 2000; 6:458–465. [PubMed: 10998375]

Landini P. Cross-talk mechanisms in biofilm formation and responses to environmental and physiological stress in *Escherichia coli*. Res Microbiol. 2009; 160:259–266. [PubMed: 19345733]

Lee JH, Lee J. Indole as an Intercellular Signal in Microbial Community. FEMS Microbiol rev. 2010; 34:426–444. [PubMed: 20070374]

Lee J, Bansal T, Jayaraman A, Bentley WE, Wood TK. Enterohemorrhagic *Escherichia coli* biofilms are inhibited by 7-hydroxyindole and stimulated by isatin. Appl Environ Microbiol. 2007; 73:4100–4109. [PubMed: 17483266]

Lee J, Zhang XS, Hegde M, Bentley WE, Jayaraman A, Wood TK. Indole cell signaling occurs primarily at low temperatures in *Escherichia coli*. ISME J. 2008a; 2:1007–1023. [PubMed: 18528414]

Lee Y, Kim Y, Yeom S, Kim S, Park S, Jeon CO, Park W. The role of disulfide bond isomerase A (DsbA) of *Escherichia coli* O157: H7 in biofilm formation and virulence. Fems Microbiology Letters. 2008b; 278:213–222. [PubMed: 18067575]

Lesic B, Lépine F, Déziel E, Zhang J, Zhang Q, Padfield K, Castonguay MH, Milot S, Stachel S, Tzika AA, Tompkins RG, Rahme LG. Inhibitors of pathogen intercellular signals as selective anti-infective compounds. PLoS Pathog. 2007; 3:1229–1239. [PubMed: 17941706]

Ma Q, Wood TK. OmpA influences *Escherichia coli* biofilm formation by repressing cellulose production through the CpxRA two-component system. Environ Microbiol. 2009; 11:2735–2746. [PubMed: 19601955]

Matthysse AG, Deora R, Mishra M, Torres AG. Polysaccharides cellulose, poly-beta-1,6-*N*-acetyl-D-glucosamine, and colanic acid are required for optimal binding of *Escherichia coli* O157:H7 strains to alfalfa sprouts and K-12 strains to plastic but not for binding to epithelial cells. Appl Environ Microbiol. 2008; 74:2384–2390. [PubMed: 18310435]

Nataro JP, Kaper JB. Diarrheagenic *Escherichia coli*. Clin Microbiol Rev. 1998; 11:142–201. [PubMed: 9457432]

Perna NT, Plunkett G 3rd, Burland V, Mau B, Glasner JD, Rose DJ, Mayhew GF, Evans PS, Gregor J, Kirkpatrick HA, Posfai G, Hackett J, Klink S, Boutin A, Shao Y, Miller L, Grotbeck EJ, Davis NW, Lim A, Dimalanta ET, Potamousis KD, Apodaca J, Anantharaman TS, Lin J, Yen G, Schwartz DC, Welch RA, Blattner FR. Genome sequence of enterohaemorrhagic *Escherichia coli* O157:H7. Nature. 2001; 409:529–533. [PubMed: 11206551]

Potera C. Forging a link between biofilms and disease. Science. 1999; 283:1837–1839. [PubMed: 10206887]

Pratt LA, Kolter R. Genetic analysis of *Escherichia coli* biofilm formation: roles of flagella, motility, chemotaxis and type I pili. Mol Microbiol. 1998; 30:285–293. [PubMed: 9791174]

Prigent-Combaret C, Prensier G, Le Thi TT, Vidal O, Lejeune P, Dorel C. Developmental pathway for biofilm formation in curli-producing *Escherichia coli* strains: role of flagella, curli and colanic acid. Environ Microbiol. 2000; 2:450–464. [PubMed: 11234933]

Puttamreddy S, Cornick NA, Minion FC. Genome-wide transposon mutagenesis reveals a role for pO157 genes in biofilm development in *Escherichia coli* O157:H7 EDL933. Infect Immun. 2010 In press.

Reisner A, Krogfelt KA, Klein BM, Zechner EL, Molin S. In vitro biofilm formation of commensal and pathogenic *Escherichia coli* strains: impact of environmental and genetic factors. J Bacteriol. 2006; 188:3572–3581. [PubMed: 16672611]

Ren D, Bedzyk LA, Ye RW, Thomas SM, Wood TK. Differential gene expression shows natural brominated furanones interfere with the autoinducer-2 bacterial signaling system of *Escherichia coli*. Biotechnol Bioeng. 2004; 88:630–642. [PubMed: 15470704]

Rivas L, Dykes GA, Fegan N. A comparative study of biofilm formation by Shiga toxigenic *Escherichia coli* using epifluorescence microscopy on stainless steel and a microtitre plate method. Journal of Microbiological Methods. 2007; 69:44–51. [PubMed: 17239460]

Ryu JH, Beuchat LR. Biofilm formation by *Escherichia coli* O157:H7 on stainless steel: effect of exopolysaccharide and Curli production on its resistance to chlorine. Appl Environ Microbiol. 2005; 71:247–254. [PubMed: 15640194]

Saldaña Z, Xicohtencatl-Cortes J, Avelino F, Phillips AD, Kaper JB, Puente JL, Girón JA. Synergistic role of curli and cellulose in cell adherence and biofilm formation of attaching and effacing *Escherichia coli* and identification of Fis as a negative regulator of curli. Environ Microbiol. 2009; 11:992–1006. [PubMed: 19187284]

Sambrook, J.; Fritsch, EF.; Maniatis, T. Molecular Cloning: A Laboratory Manual. Cold Spring Harbor Laboratory Press; Cold Spring Harbor, NY: 1989.

Strockbine NA, Marques LR, Newland JW, Smith HW, Holmes RK, O'Brien AD. Two toxin-converting phages from *Escherichia coli* O157:H7 strain 933 encode antigenically distinct toxins with similar biologic activities. Infect Immun. 1986; 53:135–140. [PubMed: 3522426]

Tarr PI, Gordon CA, Chandler WL. Shiga-toxin-producing *Escherichia coli* and haemolytic uraemic syndrome. Lancet. 2005; 365:1073–1086. [PubMed: 15781103]

Uhlich GA, Cooke PH, Solomon EB. Analyses of the red-dry-rough phenotype of an *Escherichia coli* O157:H7 strain and its role in biofilm formation and resistance to antibacterial agents. Appl Environ Microbiol. 2006; 72:2564–2572. [PubMed: 16597958]

Wang X, Kim Y, Wood TK. Control and benefits of CP4-57 prophage excision in *Escherichia coli* biofilms. ISME J. 2009; 3:1164–1179. [PubMed: 19458652]

Wells JG, Davis BR, Wachsmuth IK, Riley LW, Remis RS, Sokolow R, Morris GK. Laboratory investigation of hemorrhagic colitis outbreaks associated with a rare *Escherichia coli* serotype. J Clin Microbiol. 1983; 18:512–520. [PubMed: 6355145]

Wells TJ, Sherlock O, Rivas L, Mahajan A, Beatson SA, Torpdahl M, Webb RI, Allsopp LP, Gobius KS, Gally DL, Schembri MA. EhaA is a novel autotransporter protein of enterohemorrhagic *Escherichia coli* O157:H7 that contributes to adhesion and biofilm formation. Environ Microbiol. 2008; 10:589–604. [PubMed: 18237301]

Yoon Y, Sofos JN. Autoinducer-2 activity of gram-negative foodborne pathogenic bacteria and its influence on biofilm formation. J Food Sci. 2008; 73:M140–147. [PubMed: 18387117]

Zogaj X, Nimtz M, Rohde M, Bokranz W, Römling U. The multicellular morphotypes of *Salmonella typhimurium* and *Escherichia coli* produce cellulose as the second component of the extracellular matrix. Mol Microbiol. 2001; 39:1452–1463. [PubMed: 11260463]

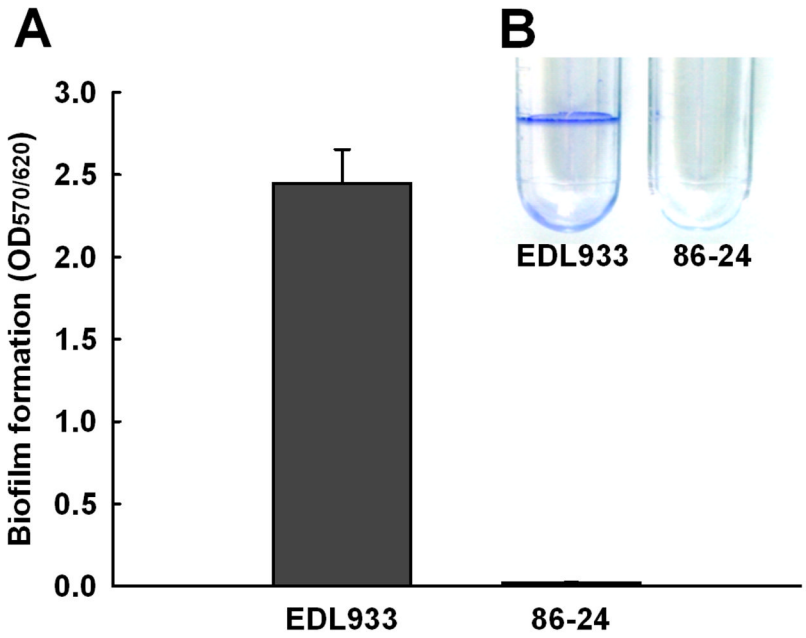

Fig. 1.

Biofilm formation of the two *E. coli* O157:H7 strains, EDL933 and 86-24, in 96-well polystyrene plates (A) and in polyethylene tubes (B) in LB medium without shaking at 37°C after 24 h. At least four independent experiments were conducted (a total 12 wells), and error bars indicate one standard deviation.

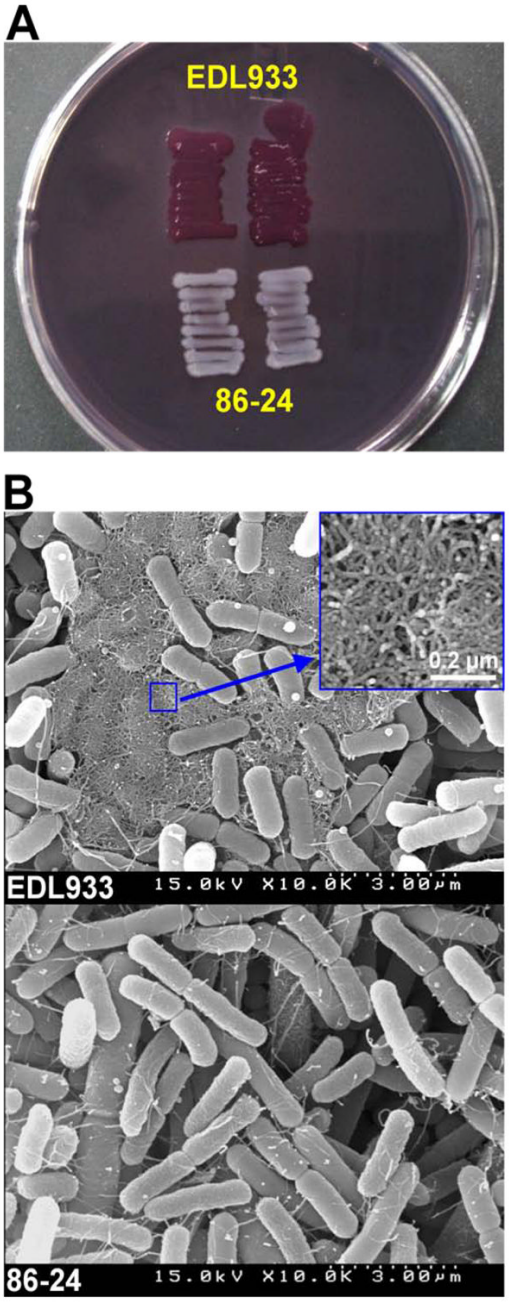

Fig. 2.

Curli formation of the two *E. coli* O157:H7 strains, EDL933 and 86-24. Curli production at 37°C after 24 h was observed using Congo red plates (A) and SEM (B). For SEM analysis, planktonic cells were grown in LB medium to turbidity of 2.0. The inset shows the magnified amorphous curli/cellulose matrix.

Table 1

Genes induced more than 6-fold for planktonic cells of EDL933 vs. 86-24. Cells were grown in LB medium at 37 °C to a turbidity of 4.0.

gene	fold change	Descriptions
Shiga-like toxin genes		
stx1B	5405	shiga-like toxin 1 subunit B
stx1A	955	shiga-like toxin 1 subunit A
Curli and cellulose genes		
csgA	49	curlin major subunit, coiled surface structures
csgB	79	minor curlin subunit precursor, similar to CsgA
csgC	84	putative curli production protein
csgD	17	putative 2-component transcriptional regulator for curli operon
csgE	24	curli production assembly transport component,
csgF	28	curli production assembly transport component
csgG	24	curli production assembly transport component
adrA	8	regulated by CsgD involved in cellulose biosynthesis
Prophage genes and unknown genes		
z1215	6	unknown protein
z1218	8	hypothetical protein
z1353	6	putative antirepressor protein of cryptic prophage CP-933M
z1354	9	putative endopeptidase of cryptic prophage CP-933M
z1362	6	unknown protein encoded by cryptic prophage CP-933M
z1364	6	unknown protein encoded by cryptic prophage CP-933M
z1373	23	unknown protein encoded by cryptic prophage CP-933M
z1443	362	unknown protein encoded by bacteriophage BP-933W
z1444	1911	putative serinethreonine kinase encoded by bacteriophage BP-933W
z1445	10,809	unknown protein encoded by bacteriophage BP-933W
z1446	1261	unknown protein encoded by bacteriophage BP-933W
z1448	256	regulatory protein Cro of bacteriophage BP-933W
z1469	158	putative lysozyme protein R of bacteriophage BP-933W
z1663	6	unknown protein
z1811	137	putative tail component encoded by prophage CP-933N
z1921	6	unknown protein encoded by prophage CP-933X
z1957	832	transposase for IS629
z2112	37	putative ClpP-like protease encoded within prophage CP-933O
z2113	32	unknown protein encoded within prophage CP-933O
z2114	891	unknown protein encoded within prophage CP-933O
z2115	16	unknown protein encoded within prophage CP-933O
z2116	832	unknown protein encoded within prophage CP-933O
z2117	30	unknown protein encoded within prophage CP-933O
z3083	69	putative tail fiber component M of prophage CP-933U
z3341	147	unknown protein encoded within prophage CP-933V

gene	fold change	Descriptions
z3342	69	unknown protein encoded within prophage CP-933V
z3347	147	unknown protein encoded within prophage CP-933V
z3348	169	unknown protein encoded within prophage CP-933V
z3357	549	putative regulatory protein CII of prophage CP-933V
z3388	208	unknown protein
z5148	6	unknown protein
z5878	69	putative integrase
z5881	338	unknown protein
z5882	42	unknown protein
z5883	7	unknown protein
z5884	91	unknown protein
z5885	13	putative resolvase
z5886	2195	unknown protein
z5887	16	unknown protein
z5888	119	unknown protein
z5889	119	unknown protein
ybcK	6	unknown protein
ybgS	8	unknown protein
yccT	13	unknown protein
yhiM	9	unknown protein
yibH	8	unknown protein
yohC	6	unknown protein
Other genes		
aidB	6	putative acyl coenzyme A
appB	12	probable third cytochrome oxidase, subunit I
appC	12	probable third cytochrome oxidase, subunit I
prpB	23	putative phosphonomutase 2
prpC	17	putative citrate synthase; propionate metabolism
prpD	21	hypothetical protein
prpE	18	putative propionyl-CoA synthetase
rpoS	11	RNA polymerase, sigma S (sigma38) factor
ssuA	28	iphatic sulphonate binding protein precursor
tfaR	9	Rac prophage

Table 2

Genes repressed more than 6-fold for planktonic cells of EDL933 vs. 86-24. Cells were grown in LB medium at 37 °C to a turbidity of 4.0.

Gene	fold change	Descriptions
Prophage genes and unknown genes		
intT	−91	IntT, integrase for prophage CP-933T
z2967	−128	unknown protein encoded by prophage CP-933T
z2968	−5405	unknown protein encoded by prophage CP-933T
z2969	−1261	unknown protein encoded by prophage CP-933T
z2970	−169	putative regulator for prophage CP-933T
z2971	−8	unknown protein encoded by prophage CP-933T
z2972	−8	unknown protein encoded by prophage CP-933T
z2973	−64	unknown protein encoded by prophage CP-933T
z2974	−23	unknown protein encoded by prophage CP-933T
z2976	−79	unknown protein encoded by prophage CP-933T
z2977	−7	unknown protein encoded by prophage CP-933T
z2979	−12	putative stabilitypartitioning protein encoded within prophage CP-933T
z2980	−17	putative stabilitypartitioning protein encoded within CP-933T
z2983	−15	putative tail fiber assembly protein of prophage CP-933T
z2984	−74	putative serine acetlyltransferase of prophage CP-933T
z2986	−37	putative tail fiber protein of prophage CP-933T
z2987	−34	putative tail fiber component of prophage CP-933T
z2988	−9	putative tail fiber protein component of prophage CP-933T
z2989	−11	unknown protein encoded by prophage CP-933T
z2990	−39	putative tail fiber component of prophage CP-933T
z2991	−39	putative tail sheath protein of prophage CP-933T
z2992	−34	putative tail assembly protein of prophage CP-933T
z2994	−315	unknown protein encoded by prophage CP-933T
z3271	−8	unknown protein
z5102	−6	unknown protein
z5111	−6	unknown protein
ydfV	−23	unknown protein, Qin prophage
Indole related genes		
trpD	−12	anthranilate synthase component II
trpE	−15	anthranilate synthase component I
trpL	−11	*trp* operon leader peptide
mtr	−13	tryptophan-specific transport protein
Other genes		
dxs	−9	deoxy-xylulose-P synthase
nlpA	−28	lipoprotein-28